

## Low temperature oxidation of CO over gold based catalysts

P. Sangeetha\*

*Center for Nanomaterials, Materials Chemistry Division, School of Advanced Sciences  
VIT University, Vellore.*

*E-mail: sangeetha.p@vit.ac.in*

### Abstract

Au catalysts supported on CeO<sub>2</sub> were prepared by deposition-precipitation method. CeO<sub>2</sub> was prepared by incipient-wetness impregnation with aqueous solution of Ce(NO<sub>3</sub>)<sub>3</sub> on TiO<sub>2</sub>. The catalysts were characterized by BET and XRD. Low temperature oxidation of CO was carried out in a fixed bed reactor. The surface area of Au/CeO<sub>2</sub> catalysts were in the range between 50 and 110 m<sup>2</sup>/g. No definite Au peaks in XRD patterns of the Au/CeO<sub>2</sub> samples, suggesting that the particle size of Au was too small to be detected. TEM images show that the particle sizes of CeO<sub>2</sub> were about 20 nm and the Au particle diameters were < 5 nm with narrow distribution. The high activity on Au/CeO<sub>2</sub> catalyst was attributed to the synergistic effects of high surface area, coexistence of metallic and oxidized gold species within nano gold particle and further due to minor portion of Ce<sup>3+</sup> species in reducible cerium oxide support and well crystalline nano cerium oxide support.

**Keywords:** Au, CeO<sub>2</sub>, pH, deposition-precipitation, CO oxidation.

### 1. Introduction

Gold has been known to be catalytically inactive; however, it has been recently discovered that, when dispersed as ultrafine particles, gold exhibits an extraordinary high activity in many reactions, in particular, in CO oxidation at low temperatures. Gold exhibits a high catalytic activity when it is deposited as nanoparticles on the metal-oxide supports [1-3]. Supported nanogold catalysts have been regarded as extremely active catalysts to oxidize CO at low temperatures [4]. The suitable supports are the metal oxides which could be partially reduced, such as TiO<sub>2</sub>, Fe<sub>2</sub>O<sub>3</sub>, and Co<sub>3</sub>O<sub>4</sub>.

Ceria has been regarded as one of the most important components in many catalytic systems due to its remarkable redox properties. Nevertheless, until recently, CeO<sub>2</sub> is not recognized as an excellent support for gold catalyzed CO oxidation [5]. CeO<sub>2</sub> has been of wide interest for decades because of its important applications including three way catalysts for automotive emission control. CeO<sub>2</sub> is one of the most thermally stable compounds; under various redox conditions, the oxidation state of the cation

may vary between +3 and +4. Its distinct defect chemistry and the ability to exchange lattice oxygen with the gas phase result in an oxide with unique catalytic properties [5], including the promotion of metal dispersion, enhancement of the catalytic activity at the metal– support interface sites, and promotion of CO removal through oxidation using lattice oxygen. CeO<sub>2</sub> has been used as the support for Pt, Pd, Rh and CuO [6-8]. During the past years CeO<sub>2</sub> has been used as a support towards CO oxidation or selective oxidation. [9] Zhou et al. [10] reported the synthesis of nano single-crystalline CeO<sub>2</sub> particles by the precipitation method and Carrettin et al. [11] reported that 2.8% Au loaded on nanocrystalline CeO<sub>2</sub> exhibited extra high activity by 2 orders of magnitude than 1.5% Au/TiO<sub>2</sub> and 5% Au/Fe<sub>2</sub>O<sub>3</sub> catalysts. A notable study by Corma and his co-workers showed that greatly improved catalysts can be achieved by using a nanocrystalline form of CeO<sub>2</sub> (average primary crystallite size ca. 3–5 nm). However, the effects of preparation methods of CeO<sub>2</sub> on the activity of Au/CeO<sub>2</sub> have not been studied extensively.

The synthesis of highly dispersed small gold particles is highly sensitive towards the preparation method. Coprecipitation, impregnation and deposition-precipitation are the most commonly used methods to synthesize gold catalysts supported on metal oxide. The preparation method which can be applied to the widest range of different support materials is the deposition-precipitation. Beside the preparation method also the synthesis conditions, like pH value during precipitation, temperature of calcination and

the pretreatment conditions (air, vacuum, hydrogen). It has been reported that deposition-precipitation has got a higher activity [12]. In this study, Au loaded on CeO<sub>2</sub> was prepared by deposition-precipitation method and further low metal loading exhibited a high CO activity.

## 2. Experimental

### 2.1 Catalyst Preparation

Cerium oxide support was prepared by precipitation method. Cerium nitrate (Ce(NO<sub>3</sub>)<sub>3</sub>·6H<sub>2</sub>O) was dissolved in distilled water (0.1 mol in 200 ml distilled water). The solution was added dropwise (10 ml/min) to an aqueous solution of NH<sub>4</sub>OH under vigorous stirring with a fixed value of pH between 8 and 11. After aging for 2 h at room temperature, the yellow precipitate was filtered and dried at 80 °C overnight. The cerium oxide was then heated between 120 and 400 °C for 4 h. Nanosized CeO<sub>2</sub> with light yellow color was obtained.

Au/CeO<sub>2</sub> catalyst was synthesized by deposition-precipitation method. HAuCl<sub>4</sub> was added dropwisely (10 ml/min) into the solution with CeO<sub>2</sub> under vigorous stirring. The temperature of the solution was maintained at 60 °C. NH<sub>4</sub>OH was used to adjust pH value at 8.5. After aging for 2 h, the precipitate was filtered and washed with distilled water at 60°C to remove residual Cl<sup>-</sup> and then dried at 80°C overnight. Finally, the catalysts were heated at

180°C for 4 h and the purple Au/CeO<sub>2</sub> catalysts were obtained.

### 2.2. Characterization

X-ray diffraction (XRD) patterns were obtained on a Siemens D500 powder diffractometer with CuK  $\alpha$  radiation (1.5405 Å) operated at 40 kV and 30 mA. All the catalysts were scanned over 20–80 degrees at a rate of 0.05 degree/min, in order to determine the identity of any phase present. The surface areas of the samples were measured using a Micromeritics ASAP 2010 by Brunauer–Emmett–Teller (BET) method for relative pressures in the range P/P<sub>0</sub> between 0.05 and 0.2. Prior to the experiments, the samples were dehydrated at 100 °C until the vacuum pressure was below 5 µmHg. d spectrometer was operated at 23.5 eV pass energy and the base pressure in the analyzing chamber was maintained on the order of 10<sup>-9</sup> Torr.

### 2.3 Catalytic activity

Catalytic activity was measured using a fixed bed continuous flow reactor at room temperature. A sample was placed in a glass tube, and then a reactant gas flow (1 vol. % CO in air) was admitted in into the reactor. About 0.06 g (bulk density = 1.515 cm<sup>3</sup>) Au/CeO<sub>2</sub> catalyst sample was placed in a glass tube reactor. The flow rate of 50 ml/min was used for all the experiments. No treatment was applied before the test. Quantitative analysis of CO and CO<sub>2</sub> was performed by a gas chromatography with TCD using argon as the carrier gas. A CO analyzer (Industrial Scientific Corp., model T82) with was used to analyze the CO concentration in the effluent down to 1 ppm.

The CO conversion and CO selectivity were calculated using the following equations:

The CO conversion was calculated based on the CO consumption as follows:

$$\% \text{ of conversion of } CO = \frac{[CO]_{in} - [CO]_{out}}{[CO]_{in}} \times 100 \quad (1)$$

### 3. Results and Discussion

#### 3.1 Characterisation

The preparation parameters and specific surface area of CeO<sub>2</sub> supports is shown in Table 1. Zou et al. [14] has reported the specific surface area of CeO<sub>2</sub> nanoparticles (about 4 nm) decreased from 170 m<sup>2</sup>/g to 90 m<sup>2</sup>/g while the calcined temperature was increased from 150 °C to 500 °C. In this study, there is no obvious relation between the specific surface areas and the calcination temperatures for CeO<sub>2</sub> samples synthesized between pH 8 and 10. CeO<sub>2</sub> samples synthesized at pH=11, the specific surface area decreased from 89 m<sup>2</sup>/g to 52 m<sup>2</sup>/g while the calcined temperature was increased from 200 °C to 400 °C. In precipitation process, the thermodynamics of reaction system and nucleation kinetics are affected by the ionic equilibrium of the supersaturated solution. Chen et al. [15] has reported the effects of alcohol/water on the properties of CeO<sub>2</sub> nanoparticles by precipitation method. The results indicated that the surface area of CeO<sub>2</sub> nanoparticle was increased to 95 m<sup>2</sup>/g and 214 m<sup>2</sup>/g for 20% methanol/water and 67% ethylene glycol/water solution, respectively. In this study, the surface areas of the samples prepared at pH 10 are greater than those at other synthesis conditions. The cerium oxide obtained at pH 10 and heating at 200 °C showed the largest surface area of 104 m<sup>2</sup>/g.

As shown in Figures 1-3, all CeO<sub>2</sub> samples showed XRD peaks at 2θ 28.5° (111), 2θ 33.1° (200), 2θ 47.5° (220), and 2θ 76.7° (311) which are well consisted with cubic fluorite (Fm3m, 225) structured CeO<sub>2</sub> (JCPDS 43-1002), indicating the well crystalline structure in all synthesized CeO<sub>2</sub> samples. The lattice parameters and crystallite sizes of CeO<sub>2</sub> samples are listed in Table 2. The lattice parameters  $d_{h,k,l}$  were calculated by Bragg's law :

$$d_{h,k,l} = \frac{\lambda \cdot \sqrt{h^2 + k^2 + l^2}}{2 \cdot \sin \theta_{h,k,l}} \quad (2)$$

The crystallite size,  $G$ , was calculated by the Scherrer's equation:

$$G = \frac{0.9 \cdot \lambda}{B_{h,k,l} \cos \theta_{h,k,l}} \quad (3)$$

where  $\lambda$  is the wavelength of Cu K<sub>α</sub> = 0.154 nm,  $\theta_{h,k,l}$  is Bragg angle of peak (111) at 28.5°, and  $B$  is the full-width at half maximum (FWHM) of peak (111) which was carefully determined by least-square fitting of Gaussian function. Lattice expansion of cubic fluorite cerium oxide nanoparticles has been reported by Zhang et al. [16] which demonstrated that the lattice parameter of CeO<sub>2</sub> particles increased from 5.4087 Å (bulk) to 5.4330 Å with decreasing particle size. The lattice expansion of small CeO<sub>2</sub> particles (< 20 nm) were attributed to oxygen vacancies and contribution of Ce<sup>3+</sup> ions. In this study, the lattice parameters were slightly greater than those of bulk CeO<sub>2</sub> crystallite. The lattice expansion of CeO<sub>2</sub> crystallite might be attributed to the size reduction of CeO<sub>2</sub> nanoparticles which were about 8-13 nm as calculated from XRD patterns. Fig. 1

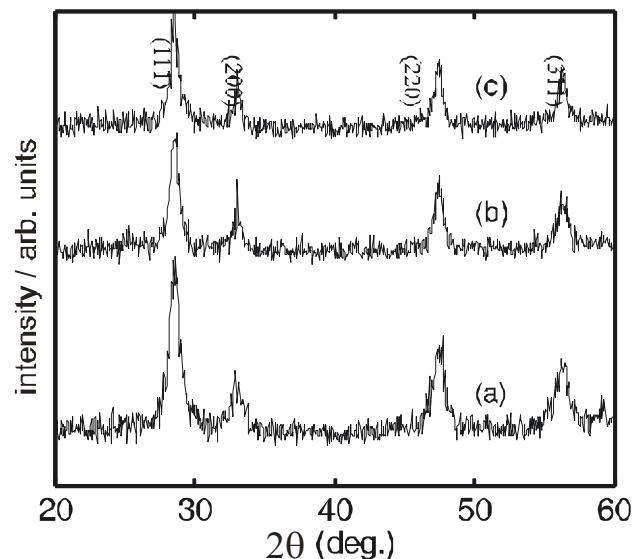


**Fig. 1** : XRD patterns of 3% Au/CeO<sub>2</sub> catalysts, where CeO<sub>2</sub> supports were synthesized at different pH and heated at 200 °C. (a) 3% Au/C9-200 (b) 3% Au/C10-200 (c) 3% Au/C11-200.

shows the XRD patterns of CeO<sub>2</sub> samples prepared at different pH values. As shown in the figure, no obvious relationship between pH value of preparation solution and the CeO<sub>2</sub> crystallite size. However, the crystallite size of CeO<sub>2</sub> decreased with increasing calcination temperature (Fig. 2). No definite Au peaks showed in the XRD patterns of the Au/CeO<sub>2</sub> samples, suggesting that the particle size of Au was too small to be detected. However, in Fig. 3, the peak intensity of CeO<sub>2</sub> samples increased after loading gold.

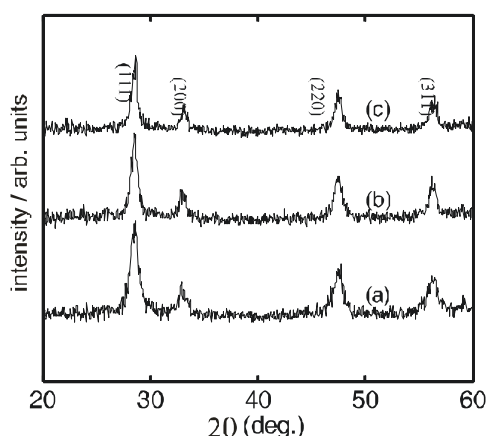


**Fig. 2** : XRD patterns of 3% Au/CeO<sub>2</sub> catalysts where CeO<sub>2</sub> was synthesized at pH of 9 and heated at different temperatures. (a) 3% Au/C9-200 (b) 3% Au/C9-300 (c) 3% Au/C9-400.

### 3. 2 Catalytic Activity

The effect of pH value of synthesis mixtures on the CO conversion of Au/CeO<sub>2</sub> catalysts are given in Fig.4. As shown in the figure, 3% Au/C10-200 gave the highest activity of CO oxidation. The CO conversion was held at 100 % for more than 4 h. The conversion was 80% on 3% Au/C11-200, whereas 3% Au/C9-200 shows the lowest activity. The results indicated that the activity reached a maximum on the catalyst with the largest surface area. The 3% C11-200 and 3% C9-200 samples had similar surface area (Table 1). The higher activity of 3% Au/C11-200 might be attributed to (i) better crystalline 3% Au/C11-200 (Table 2), the lower surface concentration of Ce<sup>3+</sup> species (Table 3) Further, since the CO conversion on the 3%

Au/C10-200 sample reached 100 %, a series of low Au loading catalysts supported on CeO<sub>2</sub> synthesized at pH of 10 were further studied. As shown in Fig. 5 it was observed that 100% conversion of CO was obtained at room temperature over 90 min on stream on 1% Au/C10-400 catalyst.

**Table 1 : Preparation conditions and surface areas of CeO<sub>2</sub> supports**

CeO <sub>2</sub> samples	pH value in precipitation of CeO <sub>2</sub>	Heating Temp. (°C)	S <sub>BET</sub> (m <sup>2</sup> /g)
C8-120	8	120	48
C8-200	8	200	59
C8-300	8	300	59
C8-400	8	400	72
C9-120	9	120	70
C9-200	9	200	82
C9-300	9	300	72
C9-400	9	400	76
C10-120	10	120	64
C10-200	10	200	104
C10-300	10	300	76
C10-400	10	400	100
C11-200	11	200	89
C11-300	11	300	76
C11-400	11	400	52

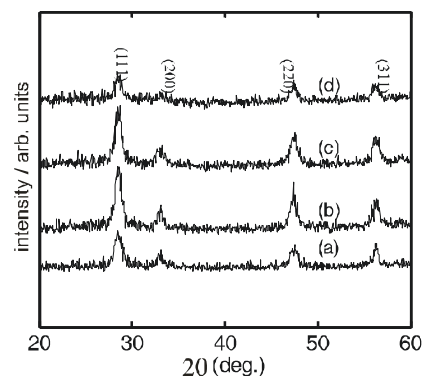


**Fig. 3** : XRD patterns of 1% Au/CeO<sub>2</sub> catalysts where CeO<sub>2</sub> support was synthesized at pH 10 and heated at 200 °C. (a) C10-200 (b) 1% Au-120/C10-200 (c) 1% Au/C10-200 (d) 1% Au/C10-200 after reaction.

Effects of crystalline of supports of supported-gold catalyst remain controversy due to different gold-support interactions, preparation process and application in different reactions. Tabakova et al. [16] reported that gold supported on well crystallized  $\text{Fe}_2\text{O}_3$  and  $\text{ZrO}_2$  exhibited higher catalytic activities than those on amorphous or not well crystallized supports. Tabakova et al. [17] reported that for  $\text{Au/CeO}_2$  supports prepared by deposition precipitation and a modified version of deposition-precipitation methods, there were no significant relations between crystallinity and water-gas shift activity because both  $\text{CeO}_2$  supports were highly crystalline. In this study, all  $\text{CeO}_2$  supports were highly crystalline. For the samples supported on C10-200, the crystallite size of 1%  $\text{Au/C10-200}$  calcined at  $180^\circ\text{C}$  was larger than 1%  $\text{Au-120/C10-200}$  catalyst calcined at  $120^\circ\text{C}$  after loading gold (Table 2).

**Table 2. Lattice parameters and crystallite sizes of  $\text{Au/CeO}_2$  samples.**

	Lattice parameter ( $\text{\AA}$ )	Crystallite Size (nm)
3% $\text{Au/C9-200}$	5.4159	8.79485
3% $\text{Au/C9-300}$	5.4194	10.1339
3% $\text{Au/C9-400}$	5.4134	12.2814
3% $\text{Au/C10-200}$	5.4170	9.8601
3% $\text{Au/C11-200}$	5.4178	9.0999
1% $\text{Au-120/C10-200}$	5.4257	8.5848
1% $\text{Au/C10-200}$	5.4209	9.2431
1% $\text{Au/C10-400}$	5.4221	9.5887

The activity test shown in Fig. 10 indicated that the 1%  $\text{Au/C10-200}$  exhibited a higher activity than 1%  $\text{Au-120/C10-200}$ . Moreover, as presented in Fig. 3 (d), the low (111) peak intensity of 1%  $\text{Au/C10-200}$  sample after 2h reaction indicated the crystalline of  $\text{CeO}_2$  was decreased.

Setiabudi et al. [18] reported the effect of  $\text{CeO}_2$  on  $\text{NO}_x$  oxidation, the storage and dispersion of “active oxygen” on  $\text{CeO}_2$  had a significant potential to accelerate the  $\text{NO}_x$  oxidation conversion. The initial  $\text{Ce}^{4+}$  concentration of 1%  $\text{Au/C10-200}$  decreased about 6% while the conversion rate decade about 3% after 2h reaction which provided another evidence of correlations between the  $\text{Ce}^{4+}$  concentration and the catalytic behavior.

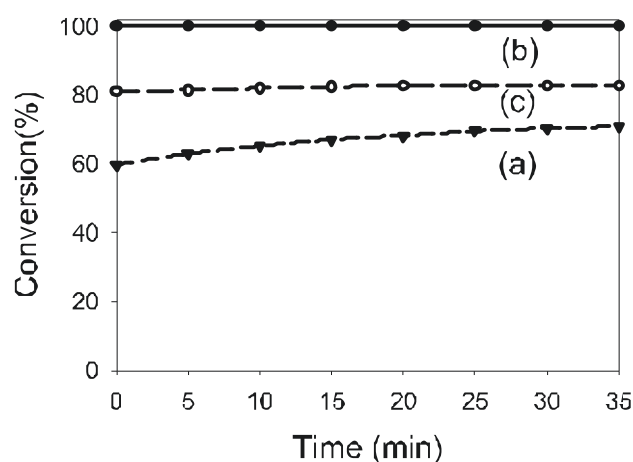


**Fig. 4 :** The conversion of 3 wt. %  $\text{Au/CeO}_2$  catalysts. (a) 3%  $\text{Au/C9-200}$  (b) 3%  $\text{Au/C10-200}$  (c) 3%  $\text{Au/C11-200}$ . (Sample weight 76 mg, and the flow rate is 50 ml/min).

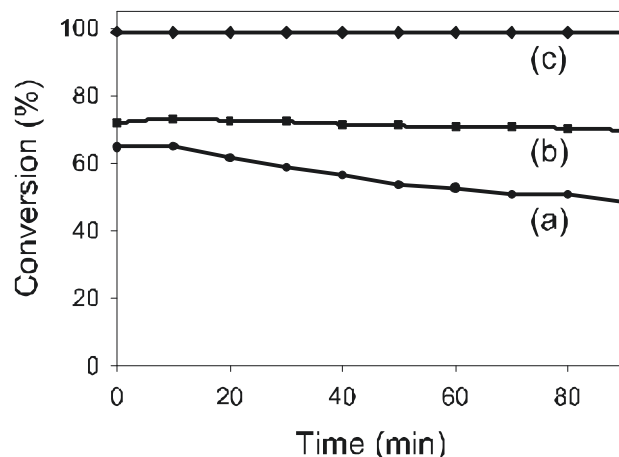


**Fig. 5 :** The conversion of 1 wt.%  $\text{Au/CeO}_2$  catalysts, (a) 1%  $\text{Au-120/C10-200}$  (b) 1%  $\text{Au/C10-200}$  (c) 1%  $\text{Au/C10-400}$ .

The catalytic properties of  $\text{Au}^0/\text{Au}$  nanoparticles were reported by Cuenya et al. [19] which demonstrated that the presence of the stabilization of  $\text{Au}^{3+}$  shell surrounding a metallic gold nanoparticle

core was a significant role of electrocatalytic activity for CO oxidation. In this study, the activity of 1% Au/C10-400 catalyst with coexistence metallic and oxidized gold species was higher than that of 1% Au/C10-200 catalyst with metallic gold state. Accordingly, the high activity of 1% Au/C10-400 sample is attributed to the synergistic effects of high surface area, coexistence of metallic and oxidized gold species within nano gold particle, minor portion of  $\text{Ce}^{3+}$  species in reducible cerium oxide support and well crystalline nano cerium oxide support.

Table 3 : Surface Concentration	
	Surface concentration of Ce(IV) (%)
3% Au/C9-200	77.9
3%Au/C10-200	83.6
3%Au/C11-200	80.0
1%Au/C10-200	82.2
1%Au/C10-200 after reaction	77.1
1%Au/C10- 400	84.4

#### 4. Conclusion

Cerium-oxide supported gold catalysts prepared by deposition-precipitation method were tested for the low temperature oxidation of CO. 1 wt. % Au loaded on  $\text{CeO}_2$  support prepared at pH 10 and calcined at  $400^\circ\text{C}$  exhibited the highest activity in CO oxidation which was held at 100 % for more than 4 h. The high activity of Au/ $\text{CeO}_2$  catalyst is attributed due to the synergistic effects of high surface area ( $> 100 \text{ m}^2/\text{g}$ ), coexistence of  $\text{Au}^0$  and  $\text{Au}^{3+}$  species within nano gold particle ( $< 5 \text{ nm}$ ), minor portion of  $\text{Ce}^{3+}$  species in reducible cerium oxide support and well crystalline nano cerium oxide support ( $\sim 20 \text{ nm}$ ).

#### References

- [1] Haruta, M. Size- and support-dependency in the catalysis of gold. *Catal. Today* 1997, 36, 153–166.
- [2] Bond, G. C.; Thompson, D. T. Catalysis by Gold. *Catal. Rev.-Sci. Eng.* 1999, 41, 319–388.
- [3] Haruta, M. Novel catalysis of gold deposited on metal oxides. *Catal. Surv. Jpn.* 1997, 1, 61–73.
- [4] Haruta, M.; Tsubota, S.; Kobayashi, T.; Kageyama, H.; Genet, M. J.; Delmon, B. Low-temperature oxidation of CO over gold supported on  $\text{TiO}_2$ ,  $\text{R-Fe}_2\text{O}_3$ , and  $\text{Co}_3\text{O}_4$ . *J. Catal.* 1993, 144, 175–192.
- [5] G.C. Bond, C. Louis, D.T. Thompson, Catalysis by Gold, vol. 6, Imperial College Press, London, 2006.
- [5] Trovarelli A. Catalytic properties of ceria and  $\text{CeO}_2$ - containing materials. *Catal Rev Sci Eng* 1996;38:439–520.
- [6] A. Yee, S. J. Morrison, H. Idriss, *J. Catal.* 186 (1999) 279.
- [7] A. Yee, S. J. Morrison, H. Idriss, *Catal. Today* 63 (2000) 327.
- [8] G. Avgouropoulos, T. Ioannides, C. Papadopoulou, J. Batista, S. Hocevar, H. K. Matralis, *Catal. Today* 75 (2002) 157.
- [9] L. Pino, A. Vita, M. Cordaro, V. Recupero, M. S. Hegde, *Appl. Catal. A: General* 243 (2003) 135.
- [10] Zhou XD, Huebner W, Anderson HU. Room-temperature homogeneous nucleation synthesis and thermal stability of nanometer single crystal  $\text{CeO}_2$ . *Appl Phys Lett* 2002;80: 3814–6.
- [11] Carrettin S, Concepcion P, Corma A, Nieto JML, Puentes VF. Nanocrystalline  $\text{CeO}_2$  increases the activity of Au for CO oxidation by two orders of magnitude. *Angew Chem Int Ed* 2004;43:2538–40.

- [12] A. Wolf, F. Schuth, *Appl. Catal. A: General* 226 (2002) 1.
- [13] F. Zhang, Q. Jin, S. W. Chan, *J. Appl. Phys.* 95 (2004) 4319.
- [14] X. D. Zhou, W. Huebner, H. U. Anderson, *Appl. Phys. Lett.* 80 (2002) 3814
- [15] H. I. Chen, H. Y. Chang, *Colloids Surf., A* 242 (2004) 61.
- [16] T. Tabakova, V. Idakiev, D. Andreeva, I. Mitov, *Appl. Catal. A: General* 202 (2000) 91.
- [17] T. Tabakova, F. Boccuzzi, M. Manzoli, J. W. Sobczak, V. Idakiev, D. Andreeva, *Appl. Catal. B: Environ.* 49 (2004) 73.
- [18] A. Setiabudi, J. L. Chen, G. Mul, M. Makkee, J. A. Moulijn, *Appl. Catal. B: Environ.* 51 (2004) 9.
- [19] B. R. Cuenya, S. H. Baeck, T. F. Jaramillo, E. W. Mcfarland, *J. Am. Chem. Soc.* 125 (2003) 12928.